JOURNAL OF GEOPHYSICAL RESEARCH, VOL. 104, NO. D17, PAGES 21,385–21,395, SEPTEMBER 20, 1999

Ozone in the remote marine boundary layer: A possible role for halogens

Russell R. Dickerson,[1] Kevin P. Rhoads,[1] Thomas P. Carsey,[2]
Samuel J. Oltmans,[3] John P. Burrows,[4] and Paul J. Crutzen[5]

Abstract. On the spring 1995 cruise of the National Oceanic and Atmospheric Administration research vessel *Malcolm Baldrige*, we measured very large diurnal variations in ozone concentrations in the marine boundary layer. Average diurnal variations of about 32% of the mean were observed over the tropical Indian Ocean. We simulated these observations with the Model of Chemistry in Clouds and Aerosols, a photochemical box model with detailed aerosol chemistry. The model was constrained with photolysis rates, humidity, aerosol concentrations, NO, CO, and O_3 specified by shipboard observations and ozonesondes. Conventional homogeneous chemistry, where ozone photolysis to $O(^1D)$ and HO_x chemistry dominate ozone destruction, can account for a diurnal variation of only about 12%. On wet sea-salt aerosols (at humidities above the deliquescence point), absorption of HOBr leads to release of BrCl and Br_2, which photolyze to produce Br atoms that may provide an additional photochemical ozone sink. After 8 days of simulation, these Br atoms reach a peak concentration of 1.2×10^7 cm^{-3} at noon and destroy ozone through a catalytic cycle involving BrO and HOBr. Reactive Br lost to HBr can be absorbed into the aerosol phase and reactivated. The model predicts a diurnal variation in O_3 of 22% with aerosol-derived Br reaction explaining much, but not all, of the observed photochemical loss. The lifetime of ozone under these conditions is short, about 2 days. These results indicate that halogens play an important role in oxidation processes and the ozone budget in parts of the remote marine boundary layer.

1. Introduction

In the clean marine boundary layer (MBL), where concentrations of nitrogen oxides (NO_x) are low, photochemical destruction is a major sink in the global ozone budget [e.g., *Crutzen*, 1973; *Liu et al.*, 1980; *Piotrowitz et al.*, 1989; *Thompson et al.*, 1993; *Torres and Thompson*, 1993; *Johnson et al.*, 1990]. Convective lifting of boundary layer air containing very low ozone mixing ratios can produce tropospheric columns of very low ozone [*Kley et al.*, 1996; *Kim et al.*, 1996; *Rhoads*, 1998]. Known processes contributing to the removal of ozone include photolysis to $O(^1D)$ followed by reaction with water vapor, reactions with odd hydrogen radicals (HO_x), and surface deposition. The conventional chemistry for tropospheric ozone destruction can be summarized as follows:

$$O_3 + h\nu \rightarrow O_2 + O(^1D)$$
$$O(^1D) + H_2O \rightarrow 2OH$$
$$OH + O_3 \rightarrow O_2 + HO_2$$
$$O_3 + HO_2 \rightarrow OH + 2O_2$$

Paluch et al. [1995] compared observed and simulated ozone destruction rates, and although the range of observations is substantial, they found general agreement with an effective first-order decay constant of 0.1d^{-1} for a lifetime of the order of 10 days. Such rates can be accounted for with the conventional HO_x chemistry in which ozone photolysis is the dominant sink. *Bremaud et al.* [1998] report a 20% diurnal variation in ozone and attribute it to photolysis of ozone during the day and unusual boundary layer dynamics, with entrainment of ozone from the free troposphere occurring predominantly at night.

Barrie et al. [1988] proposed a mechanism involving bromine atoms in the rapid destruction of ozone in the Arctic spring. Several investigators have addressed the possible role halogens may play in photochemical processes in the MBL [e.g., *Keene et al.*, 1990; *Pszenny et al.*, 1993; *Fan and Jacob*, 1992; *Finlayson-Pitts*, 1993; *Parrish et al.*, 1993; *McKeen and Liu*, 1993; *Graedel and Keene*, 1995; *Keene et al.*, 1996; *Ariya et al.*, 1998]. Others have inferred halogen atom concentrations of the order of 10^3 to 10^6 cm^{-3} from hydrocarbon measurements [*Singh et al.*, 1996; *Jobson et al.*, 1994, 1998; *Wingenter et al.*, 1996].

Vogt et al. [1996], *Sander and Crutzen* [1996], *and Sander et al.* [1997], using the Model of Chemistry in Clouds and Aerosols (MOCCA), have suggested a mechanism that does not require high concentrations of NO_x to produce halogen atoms. They point out that ozone is destroyed by the following cycle:

$$Br + O_3 \rightarrow BrO + O_2$$
$$BrO + HO_2 \rightarrow HOBr + O_2$$
$$HOBr + h\nu \rightarrow OH + Br$$
$$O_3 + HO_2 \rightarrow OH + 2O_2 \quad \text{net}$$

Most recently, *Hirokawa et al.* [1998] observed the formation of Br_2 from reaction of O_3 on NaBr particles in labora-

[1]Departments of Meteorology and Chemistry, University of Maryland, College Park.
[2]Atlantic Oceanographic and Meteorological Laboratory, NOAA, Miami, Florida.
[3]Climate Monitoring and Diagnostics Laboratory, NOAA, Boulder, Colorado.
[4]Institut für Umweltphysik/Fernerkundung, Universität Bremen, Bremen, Germany.
[5]Max-Planck-Institut für Chemie, Mainz, Gemany.

Paper number 1999JD900023.
0148-0227/99/1999JD900023$09.00

tory experiments, and *Spicer et al.* [1998] observed substantial amounts of Cl_2 at night, but major uncertainties remain in the origin and fate of tropospheric halogen atoms.

Here we present surface and ozonesonde measurements made aboard the National Oceanic and Atmospheric Administration (NOAA) research vessel R/V Malcolm Baldrige as part of a PRE-INDOEX(Indian Ocean Experiment) cruise on the Atlantic and Indian Oceans in February to April 1995 [*Ramanathan et al.*, 1996; *Rhoads et al.*, 1997; *Rhoads*, 1998; *deLaat et al.*, 1999]. We discuss numerical simulations performed to determine if halogen chemistry can help explain the strong diurnal variations in ozone observed.

2. Observations

From the ship, surface ozone was measured with an instrument based on UV absorption (model 300, Environics, West Willington, Connecticut). A Teflon filter, changed every few days, protected the inlet from contamination by aerosol particles. As a further precaution against interferences from soot from the ship's exhaust, the sample flow was interrupted whenever the winds were from the stern. The instrument zero, checked every few days with an ozone-destroying catalyst (Hopcalite, Mine Safety Appliances, Pittsburgh, Pennsylvania) or by turning off the sample pump, showed no diurnal variation and drifted by less than 2 ppb over the course of the experiment. Tests following the cruise showed no detectable loss of ozone on the inlet lines. Ozone detection at the Atmosphere/Ocean Chemistry Experiment (AEROCE) site in Barbados is described by *Oltmans and Levy* [1994].

Sondes, launched in early afternoon local time over the Indian Ocean, provided profiles of temperature, humidity, and ozone. Data from these electrochemical sondes were analyzed according to the method described by *Oltmans et al.* [1996]. Readings taken from the sondes immediately prior to release matched, within experimental uncertainty, those of the shipboard ozone instrument; sonde observations averaged 2.3 ppb higher with a root-mean-squared difference of 3.5 ppb.

Surface water vapor was determined with a dew point hygrometer with an estimated absolute accuracy of about 1°C or better. At these dew points, 1°C corresponds to about 6% in either vapor pressure or molecular number density. Water vapor pressure determined every 4 hours with a psychrometer agreed within 5%, on average. The relative humidity (RH) measured by sensors on the ozonesondes prior to launch was generally about 15% lower, but this may be due to weak winds and radiative heating aft of the bridge. The difference dropped to about 5% by the time the balloons were 20-40 m above the ship. For the Indian Ocean leg of the cruise, measurements of carbon monoxide (CO), nitric oxide (NO), standard meteorological variables, and the NO_2 photolysis rate coefficient are described by *Rhoads et al.* [1997]. For the Atlantic leg, only surface O_3, CO, and water vapor were measured.

3. Numerical Simulation

In MOCCA the rates of change of trace gases in the MBL (equation (1)) are regulated by gas-phase photochemical reactions, input from the free troposphere or ocean surface, dry deposition at the sea surface, and by exchange with aerosol.

$$dC_g/dt = P_g - L_g + E/Z - C_g V_d/Z - Lk_t(C_g - C_{g,eq}) \quad (1)$$

where C_g is the gas-phase concentration; P_g and L_g are gas-phase photochemical production and loss, respectively; E is the emission rate (or downward mass flux for ozone); Z is the boundary layer height; V_d is the deposition velocity; L is the liquid water content (LWC); k_t is the gas-aerosol exchange coefficient; and $C_{g,eq}$ is the gas-phase concentration in equilibrium with the aqueous phase. Over land, entrainment of air from the free troposphere into the boundary layer is faster during the daylight hours, but the effective heat capacity of the ocean surface is much greater than that of the land, and the amplitude of the diurnal variation of the MBL is damped relative to the continental boundary layer. For most of the runs shown here, we applied a constant ozone flux of 2.2 x 10^{11} molecules cm^{-2} s^{-1}.

The rates of change of concentrations of aerosol species (equation (2)) are regulated by reactions in aerosol solutions, exchange with the gas phase, and exchange of fresh and aged aerosols with the sea surface.

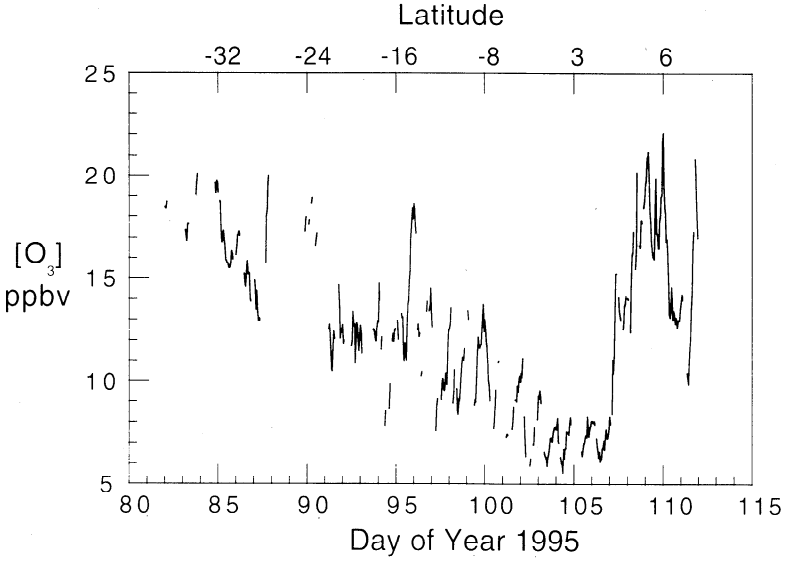

Figure 1. Variation in surface ozone with time (bottom axis) and approximate latitude (top axis) observed during the Indian Ocean leg of the 1995 cruise of the R/V *Malcolm Baldrige*.

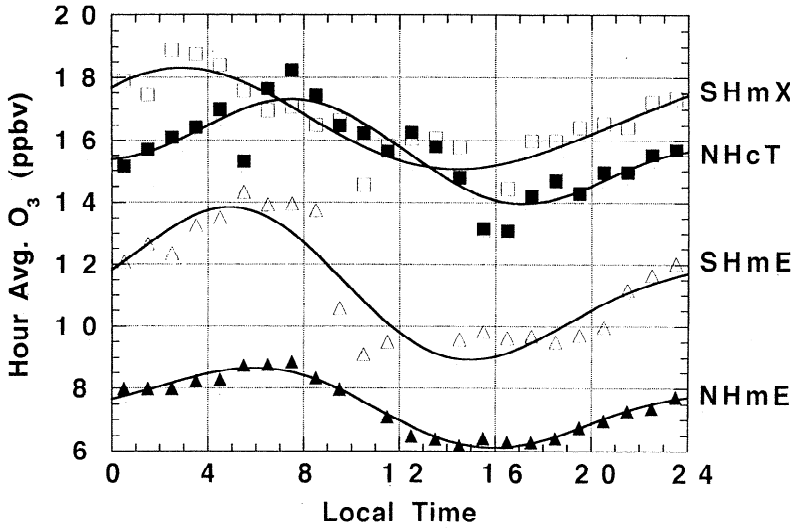

Figure 2. Mean diurnal variation in ozone observed for the four meteorological regimes encountered: Southern Hemisphere extratropics (SHmX) (34 to 22°S), Southern Hemisphere maritime equatorial (SHmE) (18 to 6°S), Northern Hemisphere maritime equatorial (NHmE) (6° S to 6° N), and Northern Hemisphere continental tropical (NHcT) (4.5°N to 9°N). Data are averages of all observations from each regime in each hourly interval. Sunrise and sunset occurred near 0600 and 1800 in the equatorial regimes. A best-fit polynomial curve is shown for each regime as a visual aid [*Rhoads et al.*, 1997].

$$dCa/dt = Pa - La + kx(Ca,0 - Ca) = Lkt(Cg - Cg,eq) \quad (2)$$

where C_a is the aerosol-phase concentration; P_a and L_a are the aerosol-phase photochemical production and loss respectively k_x is the sea surface-aerosol exchange coefficient; and $C_{a,0}$ the concentration in freshly emitted aerosol. Two types of aerosol are simulated, sea salt and sulfate.

4. Experimental Results, Indian Ocean

Rhoads et al. [1997] and *Rhoads* [1998] describe the ship track, synoptic situations, and CO and O_3 mixing ratios encountered on the cruise from Miami, Florida, to Durban, South Africa, and on to Colombo, Sri Lanka. A much more detailed set of observations was carried out on the second leg of the cruise on the Indian Ocean, so those results will be presented first.

In brief, the vessel crossed through the following four meteorological regimes: Southern Hemisphere maritime extratropics (SHmX), Southern Hemisphere maritime equatorial (SHmE), Northern Hemisphere maritime equatorial (NHmE), and Northern Hemisphere continental tropical, (NHcT). The latitudinal variations in ozone (Figure 1) and other trace species reflect the influence of these four meteorological regimes. CO jumped from about 60 to 89 ppb as the ship crossed the Intertropical Convergence Zone (ITCZ) into the meteorological Northern Hemisphere, while NO reached an average daytime mixing ratio of 5 ±2 ppt (parts per 10^{12} by volume) throughout the equatorial regions [*Rhoads et al.*, 1997], similar to previous observations in the remote MBL [e.g., *McFarland et al.*, 1979; *Emmons et al.*, 1997].

Relatively high O_3 concentrations were encountered outside the equatorial regions; most likely due to downward transport from the stratosphere or emissions from southern Africa in the SHmX regime. In the NHcT regime, increased concentrations of reactive nitrogen, CO, and other pollutants showed that photochemical smog processes had increased

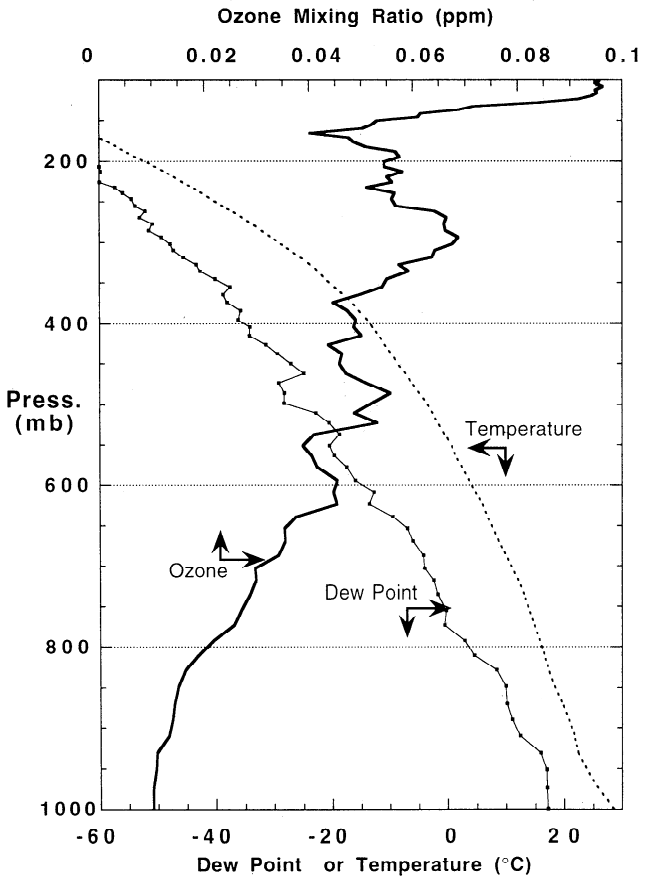

Figure 3. Average ozone results from five ozonesondes launched under NHmE conditions. Sondes were launched near 1300 local time. Note the sharp increase in ozone, decrease in water vapor, and temperature inversion at the top of the MBL around 920 mbar (800 m). Sondes measured, on average, 2.3 ppb higher ozone mixing ratios than the shipboard instrument.

ozone levels. Lowest mixing ratios were observed in the equatorial regions where transport was very slow and the air parcels reaching the ship had spent long periods over the ocean.

In the SHmE and NHmE regimes, day-to-day weather and the diurnal variation in ozone were fairly uniform. We have taken all the data from each of the four meteorological regimes and computed means for each hour (Figure 2). In the remote MBL of these regimes, conditions of very low NO_x and high water vapor lead to rapid photochemical destruction of ozone during the day, followed by replenishment from the free troposphere at night. The equatorial regimes showed the smallest concentrations but the greatest relative amplitude with average diurnal variations (maximum minus minimum over mean) of about 32%. In the NHcT regime, where NO and other ozone precursors were advected from India, competing photochemical production and destruction led to little net change in ozone with time of day.

Results from all ozonesondes launched under NHmE conditions were combined to yield an average ozone profile for this meteorological regime (Figure 3). These sondes were launched in early afternoon each day and show the increase in ozone mixing ratio above the inversion height around 800 m. At night, photochemical destruction ceases, but downward mixing continues. By sunrise each morning, surface ozone concentrations (Figure 2) nearly matched values observed in the lower free troposphere.

Table 1. Conditions for Northern Hemisphere Maritime Equatorial Regime, April 1995

Parameter	Comments	Value
Temperature, T, K	mid-MBL	298
Pressure, P, hPa	mid-MBL	950
Relative Humidity, RH, %	mid-MBL	83.5
[CO], ppb		89
[NO], ppt	noon	4
Overhead Ozone Content, Ω Dobson Units		266.5
[H_2CO], ppb	model	0.5
[NaCl], μgm^{-3}	observation range	0.3 to 3.9
[NaCl] , μgm^{-3}	model	3.73
[SO_4^{2-}], μgm^{-3}	observation range	0.2 to 2.0
[SO_4^{2-}], μgm^{-3}	model	0.92
LWC, dimensionless V/V	model sea salt	6.0×10^{-11}
LWC, dimensionless V/V	model sulfate	2.14×10^{-12}

MBL is marine boundary layer; LWC is liquid water content; V/V is volume mixing ratio. Values represent observational means unless otherwise noted.

Table 2. New Photolysis Rate Coefficients for Mid-MBL in the Cloud-Free Tropics

Coefficient	Source
$j(O_3\ ^1D) = 6.1 \times 10^{-5} \cos^2(\theta)$	*Dickerson et al.* [1982]
$j(NO_2) = 9.74 \times 10^{-3} \cos(\theta)$	set to match observations
$j(HOBr) = 0.21 \times j(NO_2)$	J. Crowley (personal communication, 1997)
$j(BrNO_3) = 8.04 \times 10^{-4} \times \cos(\theta)$	*NASA* [1997]

All coefficients have units of s^{-1}; θ is the solar zenith angle; all other rate coefficients are as in *Sanders and Crutzen* [1996], but multiplied by 1.2 to account for the cloud free conditions encountered.

5. Matching Model to Experimental Conditions

MOCCA was run with mixing ratios CO, NO, H_2O, and overhead ozone column Ω specified by the observations from the NHmE regime; model aerosol concentrations were within the range of observations (Table 1). *Sander and Crutzen* [1996] developed MOCCA for midlatitude conditions. To simulate more realistically tropical conditions encountered in PRE-INDOEX, we modified the model in several important ways: (1) photolysis rates appropriate for clear skies in the tropics, (2) reduced deposition velocities for reactive species, (3) temperature and relative humidity from the middle of the MBL, and doubled liquid water content of the particles.

Photolysis rates (Table 2) are calculated for appropriate solar zenith angles and overhead ozone column, as measured by the sondes. Calculated values of $j(NO_2)$ agreed well with shipboard actinometric observations [*Rhoads et al.*, 1997]. The ozone column above the altitude where the balloon burst (typically about 35 km) was estimated from a climatology based on solar backscattered ultraviolet (SBUV) observations [*McPeters et al.*, 1997]. The solar zenith angle dependence of $j(O_3)$ in MOCCA was modified to track $\cos^2(\theta)$, where θ is the solar zenith angle; this matches more faithfully the dependence on effective ozone column content.

For lifetimes long relative to vertical mixing within the MBL, such as the lifetime of ozone with respect to photolysis to $O(^1D)$, a rate coefficient for the middle of the MBL is more appropriate than for the surface. While there is reasonable agreement between direct measurements and models for $j(O_3)$ at Earth's surface, there is substantial uncertainty in the altitude dependence of $j(O_3)$. Rayleigh scattering increases the radiative flux, but the quantum yield falls rapidly with decreasing temperature.

Model $j(O_3)$ was set to match actinometric measurements [*Dickerson et al.*, 1982] for equivalent effective ozone column. This provides a rigorous test of the hypothesis that ozone photolysis is inadequate to explain the diurnal variation, because these photolysis rate coefficients are on the high end but within experimental uncertainty of other published direct measurements [*Bahe et al.*, 1979; *Blackburn et al.*, 1992; *Bairai and Stedman*, 1992; *Hofzumahaus et al.*, 1992; *Shetter et al.*, 1996].

We based deposition velocities on solubility and an expected vertical concentration gradient in the MBL. In a well-

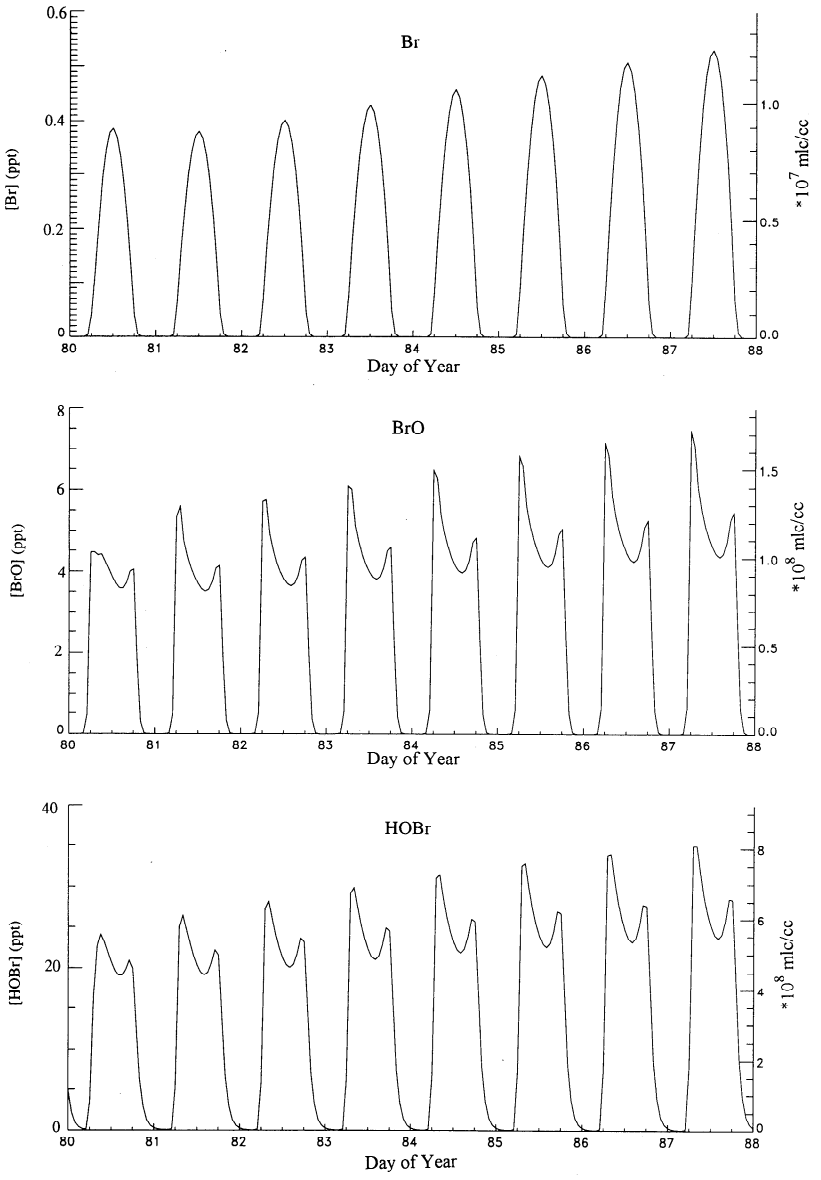

Figure 4a. Left, mixing ratios and right, concentrations of reactive bromine species for 8 days of model run. Large tic marks and numbers for the day of the year are below the beginning (0000) local solar time for each day. Note that mean concentrations rise steadily throughout the run and peak at solar noon.

mixed atmosphere, highly soluble species such as HBr have faster deposition velocities than less soluble species such as HOBr, but species with lifetimes short relative to the time for vertical mixing in the MBL form vertical concentration gradients. Lower mixing ratios near the sea surface reduce the effective deposition velocity for the MBL as a whole, as pointed out by *Sander and Crutzen* [1996]; we used the same values except for H_2O_2, HOCl, and HOBr, which we set to 0.04 cm s^{-1}.

If aerosol particles are well mixed within the MBL, then the appropriate temperature and relative humidity are those of the middle of the MBL (Table 1). This becomes especially important for aerosol LWC because it depends strongly on RH. The dew point typically remains reasonably constant with height in the MBL, but the RH increases rapidly (Figure 3). The water content of the aerosol was not measured, and MOCCA lacks the capacity to calculate LWC, so a reasonable value based on RH was specified.

The final substantive change from MOCCA as run by *Sander and Crutzen* [1996] was to double the rate of aerosol exchange with the surface 1 d^{-1}. The lifetime of sea-salt aerosol particles in the MBL is generally taken to be 1-2 days [*Erickson et al.*, 1999]; using the shorter lifetime increases the flux of fresh, halogen-rich particles, generates higher concentrations of gas-phase bromine, and brings the modeled ozone into better agreement with observations.

6. Model Results

MOCCA was run for 8 days near the equinox for 4°N latitude, corresponding to the observations in the NHmE regime. Modeled concentrations of gaseous bromine species (Figures 4a and 4b) rise steadily through the BrO_x mechanism outlined above. The model predicts substantial steady state concentrations of HOBr, BrO, and Br during the day and of BrCl and Br_2 at night. After about 2 days, average bromide

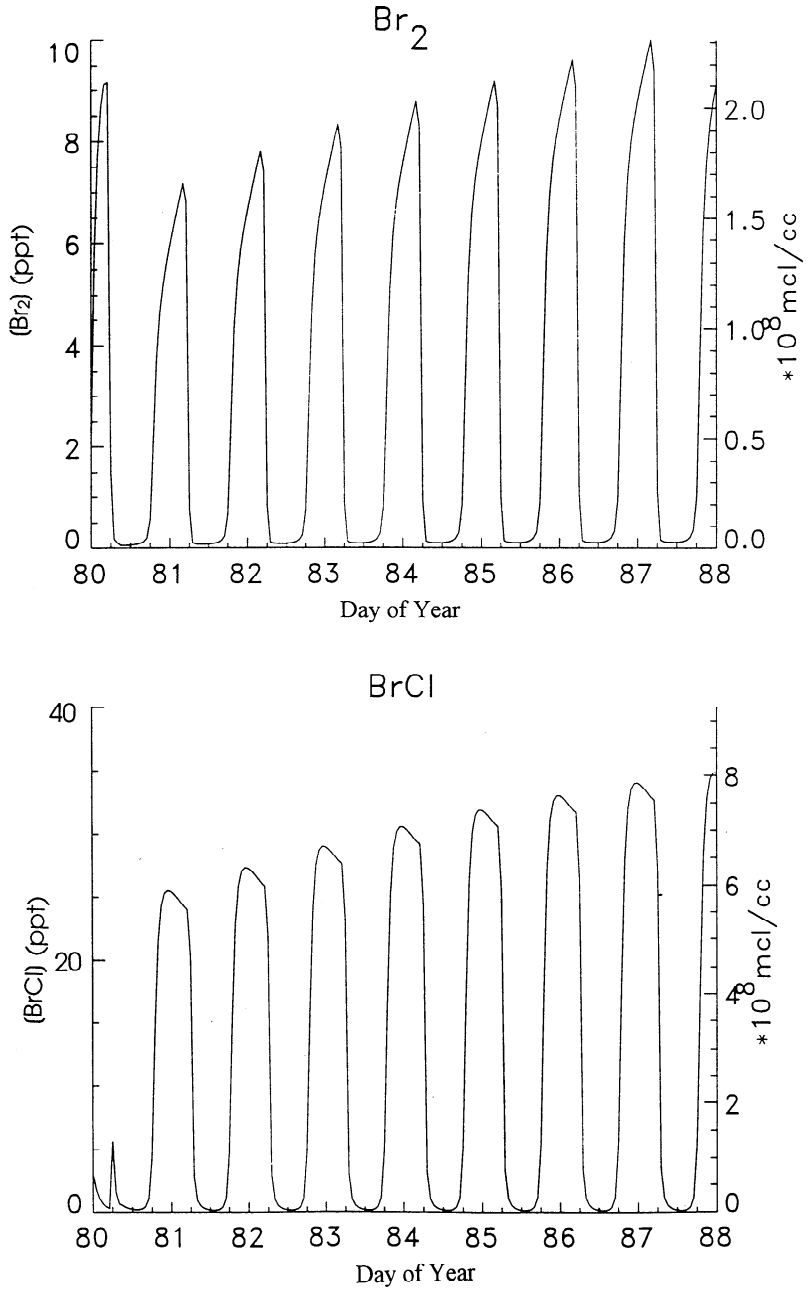

Figure 4b. Same as Figure 4a, except for gas-phase bromine reservoir species; concentrations peak at night.

(HBr + Br-) in sea-salt aerosol particles has fallen substantially from the initial concentration of 4 x 10^{-3} (Figure 4c); such Br deficits have been observed [*Sander et al.*, 1998]. As the gas-phase bromine concentration increases over the course of the 8-day run, aerosol-phase bromide concentration also increases and shows a peak during the daylight hours of about 2 x 10^{-3} *M* in the coarse aerosol and 1 x 10^{-3} *M* in the fine aerosol particles. The exchange of bromine between gas and aerosol phases gives this halogen a lifetime in the MBL longer than that of the particles themselves.

The calculated mixing ratio of ozone in the MBL (Figure 4d) shows a maximum shortly after sunrise and a minimum in midafternoon. In the run with full heterogeneous chemistry, the concentration shows a steady decrease from one day to the next. As the daily average concentration falls, the relative diurnal variation grows, as was observed from the ship in the SHmE and NHmE regimes. For control runs without aerosol chemistry, the diurnal variation was smaller and the ozone concentration was greater, even though the flux of ozone was reduced to compensate for the slower destruction.

The reactive bromine cycle in the clean MBL (Figure 5) consumes O_3 in the catalytic cycle involving Br, BrO, and HOBr. The major loss of reactive bromine is Br reaction with H_2CO (about 500 ppt in the model) to produce HBr. If this HBr deposits on the ocean, reactive bromine is lost from the atmosphere, but for the simulated conditions most of the HBr returns to the aerosol phase, from which it is re-released. In the model, daytime chlorine atom concentrations peak around

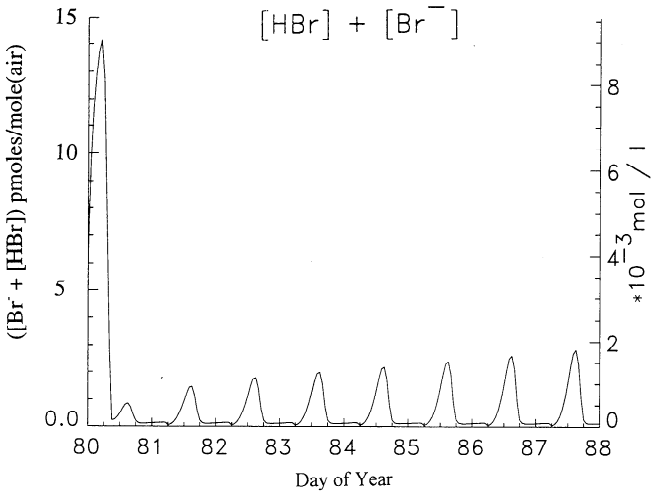

Figure 4c. Same as Figure 4a, except for bromide in the sea-salt particles. Left axis shows the mixing ratio of particulate-phase bromine in air (in equivalent parts per trillion), by volume and the right axis shows the concentration in the liquid. Note that the initial concentrations are quickly depleted and then slowly rise again as the gas-phase bromine concentration grows; the initial concentration ($4 \times 10^{-3} M$) is difficult to distinguish from the *Y*-axis because the concentration is changing so quickly. The model predicts a strong diurnal variation in bromide, with the minimum at night.

3×10^4 cm^{-3}; chlorine plays only a minor role in ozone destruction, but may represent a nontrivial sink of other species such as dimethyl sulfide (DMS) [*Keene et al.*, 1996].

Comparison of observed and calculated diurnal cycles (Figure 6) shows that aerosol-generated bromine species bring the model values closer to measurements but cannot explain the entire diurnal variation in ozone. For day 8 of the MOCCA run, with peak Br of 1.2×10^7 cm^{-3}, the calculated diurnal variation was 22%, less than the 32% measured, but substantially more than the 12% simulated with conventional chemistry, i.e., with the heterogeneous chemistry turned off. The model does reproduce the timing of the maximum near dawn and minimum in midafternoon.

The addition of the bromine mechanism does not account perfectly for the observed ozone concentrations. The model produces diurnal variations substantially in excess of those produced by conventional chemistry only for ozone mixing ratios in excess of 15 ppb. For lower ozone levels, H_2CO effectively competes with O_3 for reaction with Br. In addition, HO_2 falls off and BrO is tied up in cycles with $BrNO_3$ that do not reduce odd oxygen; these reduce the magnitude of the diurnal variation in O_3.

Observed mixing ratios of NO_2 averaged 19 ppt, and daytime NO averaged 5 ppt [*Rhoads et al.*, 1997]. For this study, the concentration and diurnal variation of ozone were insensitive to the NO emission rate as long as the peak NO concentration remained below about 8 ppt, but matching the model to observations led to some surprising results. Because heterogeneous reactions convert NO_x to nitrate very quickly, the NO emission rate in MOCCA had to be increased to 3.5×10^9 molecules cm^{-2} s^{-1} to maintain mixing ratios of a few ppt NO and about 20 ppt NO_x. Such a high surface flux implies a lifetime for NO_y of about 8 hours and conflicts with other estimates of ocean NO emissions [e.g., *McFarland et al.*, 1979; *Intergovernmental Panel on Climate Change* (*IPCC*), 1994]. There are several alternative explanations. MOCCA may overestimate the rate of conversion of NO_x to nitrate or be missing a mechanism to convert nitrate back to NO_x. Advection of pollution in the free troposphere may have led to NO_x entrainment into the MBL, or the measurement of NO_x may have suffered from an unidentified positive interference; further investigation is warranted.

Diurnal variations in dimethyl sulfide in excess of those predicted by loss due to reaction with OH have been reported [*Chin et al.*, 1996; *Suhre et al.*, 1995; *Yvon et al.*, 1996] and halogens may also play a role in the budget of marine sulfur species [*Toumi*, 1994; *Keene et al.*, 1996]. MOCCA as configured for these studies, predicted that loss of DMS to BrO would be the same magnitude as loss to OH. Our model also predicted strong diurnal variation in DMS, from 15 ppt during the day to 40 ppt at night similar in magnitude or even greater than observed diurnal cycles.

7. Sensitivity Studies

We investigated the sensitivity of our results to several model assumptions. One of the key variables is the competition between sea surface and aerosols for HBr. The rate of collision of HBr with particles depends linearly on the surface area of the particles, and high concentrations of reactive bromine can only be maintained for relatively high exchange

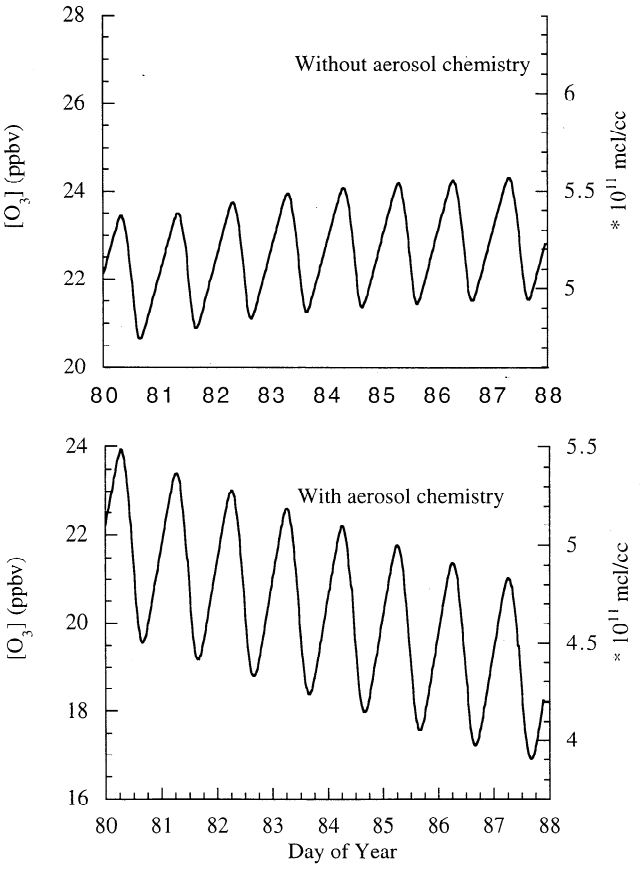

Figure 4d. Same as Figure 4a, except for ozone. Calculated concentrations shown (top) with all aerosol chemistry turned off and (bottom) including aerosol chemistry. Reactions involving bromine and sea salt particles generate lower absolute values and greater diurnal variation.

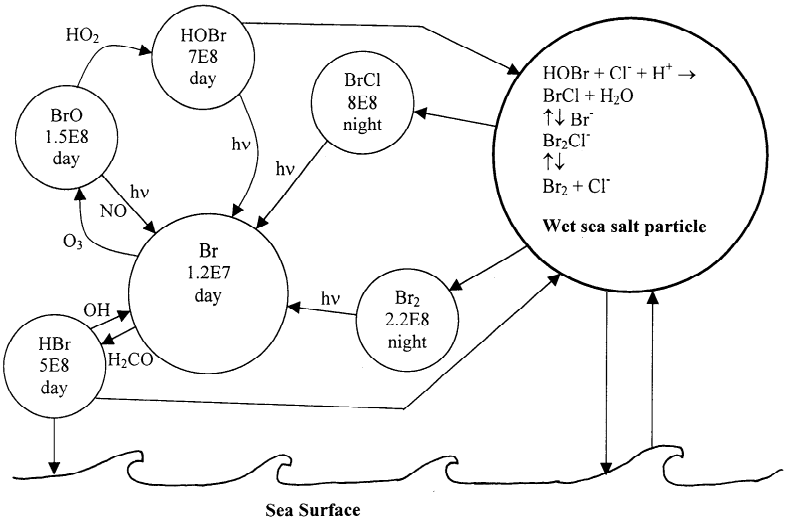

Figure 5. Schematic diagram of reactive bromine cycle in the remote marine boundary layer (MBL) showing peak concentrations (in cm^{-3}) and major pathways. Curved arrows connecting HOBr, Br, and BrO show the ozone destruction cycle. For this mechanism to serve as a major sink of ozone, the sea-salt aerosol must carry a substantial liquid water content (LWC) and sea-salt particles must effectively compete with the sea surface for HBr and HOBr.

rates and LWC. For LWC of half that used here, the diurnal variation of ozone fell from 22 to 17%. In addition, aldehydes compete with O_3 for reaction with Br, and very high formaldehyde concentrations can inhibit the catalytic O_3 destruction cycle.

The calculated diurnal variation is moderately sensitive to the amount of dry particulate matter. When the aerosol loading in the model was doubled, the diurnal variation grew to 27%; when it was halved, the diurnal variation fell to 19%. Model results were relatively insensitive to the assumed solubility of HOBr, aqueous-phase rate coefficients for Br_xCl_y species, and NO_x levels. Higher concentrations of NO_x produce $BrNO_3$ that reacts quickly on wet particles and increases active Br, but higher NO_x inhibits O_3 destruction. Results were only moderately sensitive to the rate of photolysis of HOBr; at high j(HOBr) the increased rate of Br production is counteracted by reduced aqueous-phase production of Br_2 and BrCl.

Atmospheric acidity does have a major impact on the BrO_x ozone destruction cycle. The sea-salt aerosol must be acidic, because the halogen reactions are acid catalyzed [*Vogt et al.*, 1996]. Although sea-salt particles start out alkaline, in the model runs presented here they are quickly made acidic by absorbing SO_2, H_2SO_4, or HNO_3 from ocean-emitted DMS or NO. The calculated pH is about 4.6, in the range described by *Keene et al.* [1998] and *Erickson et al.* [1999].

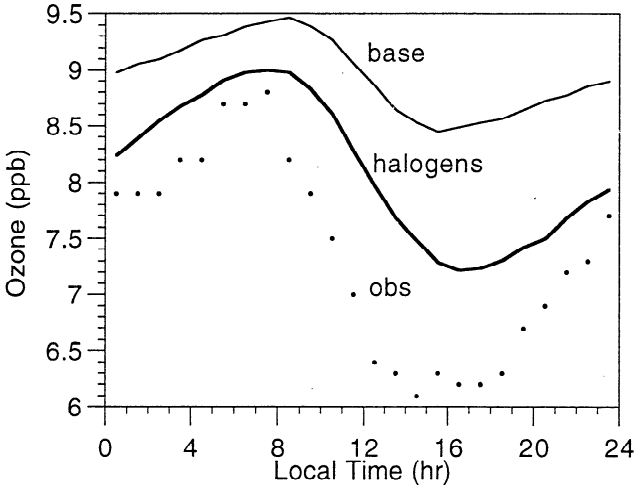

Figure 6. Average observed (dots) and calculated (lines) diurnal variations in ozone for the NHmE regime. Calculated mixing ratios are normalized and slightly offset for clarity. With conventional HO_x chemistry (base), the calculated diurnal variation is about 12%, much less than the observed 32%. When ozone destruction by reaction with halogens is added to the model, the diurnal variation rises to 22%.

8. Observations From Other Locations

If in the remote, low-latitude MBL halogen chemistry can dominate the loss of ozone, large diurnal variations should have been observed previously. *Oltmans and Levy* [1994] reported average diurnal variations of 10-12% on the island sites of Barbados (13°N), Samoa (14°S), and (in the summer months) Bermuda (32°N). Islands can alter MBL dynamics, and average diurnal variations, however, can mask periods of more extreme variability. *Oltmans* [1981] described a 4-day period at Samoa when diurnal ozone variations ranged from 25 to 45%. Examination of the ozone record from Barbados revealed a diurnal variation of 20% for a 2-week period in December 1992 when zenith angles are relatively large. *Lal et al.* [1998] also observed large ozone diurnal variations over the Indian Ocean on a cruise in 1996.

Some other cruises showed only modest diurnal variations in the tropical MBL [*Johnson et al.*, 1990; *Thompson et al.*, 1993], but changes in boundary layer depth can reduce the amplitude of the 24-hour cycle and conceal halogen chemistry. The height of the inversion increases with low-level convergence associated with falling barometric pressure. Surface heating by solar radiation, especially when winds are weak

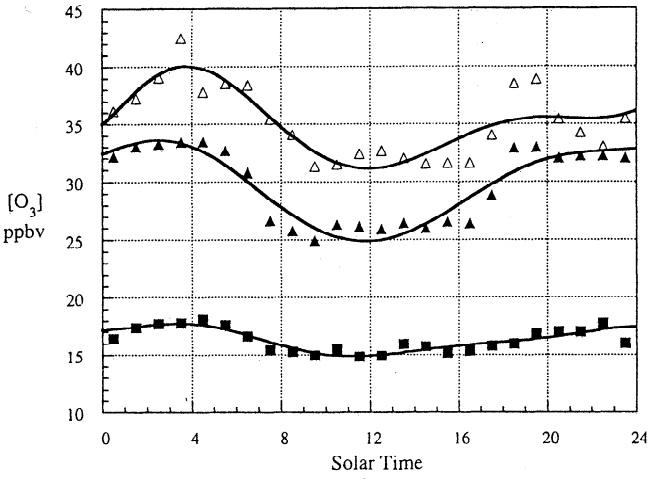

Figure 7. Mean diurnal variation in ozone observed on the Atlantic Ocean leg of the cruise February 13 to March 16 (DOY 44 to 75), 1995. In the Northern Hemisphere extratropics (open triangles), air from the North American continent was sometimes encountered, and the diurnal variation does not show a smooth day/night transition. In the Northern Hemisphere equatorial (filled triangles) regime, the diurnal variation was about 25%. In the Southern Hemisphere tropical (filled squares) regime, the diurnal variation was about 18%, although day/night transition is less clean, perhaps owing to winds carrying ozone-producing trace gases from Africa. The mean diurnal variation observed from the east (windward) side of Barbados for the time when the ship was upwind (about 500 km to the ENE) was 11 to 14%.

and the ocean's mixed layer is shallow, also expands the atmospheric boundary layer. If the depth of the MBL grows during the daylight hours, then the rate of entrainment of ozone from the free troposphere will be greater during the day than at night and counterbalance rapid photochemical ozone destruction. The diurnal variation of ozone reveals halogen chemistry most clearly when the MBL is stable for 24 hours or more and reasonably shallow; a deep MBL will dilute the aerosol chemistry and weaken the diurnal variation.

On the Atlantic leg of the cruise [*Rhoads*, 1998], strong diurnal variations were encountered in the equatorial regions, although not as strong as over the Indian Ocean (Figure 7). In the Northern Hemisphere equatorial region Julian Day or day of the year (DOY) 49-63, ozone mixing ratios reached a broad minimum around 26 ppb during daylight hours and climbed to about 33 ppb at night for a diurnal variation of about 25%. In the Southern Hemisphere equatorial region (DOY 64-70), the diurnal variation was less distinct, but the day/night difference was around 18%. The weaker diurnal variations over the Atlantic may result from greater solar zenith angles at the time of the observations or from shorter time to build up halogens. Back trajectories show that on the Atlantic cruise the air had less time to develop marine character than on the Indian Ocean cruise [*Rhoads*, 1998].

Ozone concentrations measured at the island site on Barbados (13°N) at the time of the cruise were near the climatological mean for February [*Oltmans and Levy*, 1994] and fell within the range of observations measured from the ship at the point of its closest passing (about 500 km upwind) on DOY 55-57 (Figure 7). The diurnal variation in ozone measured near Barbados for this time was 11 to 14%.

9. Discussion and Conclusions

Over the equatorial Indian Ocean ozone, concentrations were low and the diurnal cycle was large. Conventional HO_x chemistry cannot account for such variations; ozone photolysis rate coefficients nearly triple current estimates are required. The addition of reactive bromine chemistry can produce a 22% diurnal variation in ozone and bring theory closer to observation. The version of MOCCA run for these studies had no iodine chemistry, and aerosol-activated iodine photochemistry may also contribute to ozone destruction in the MBL [*Ariya et al.*, 1998; *Vogt et al.*, 1999].

MOCCA predicts substantial amounts of reactive bromine for clean marine conditions where there has been no rain for several days. Clear skies provide adequate sunshine for photochemistry, inhibit rapid intermixing of MBL and free tropospheric air, and allow buildup of soluble bromine species such HBr. These results are robust with respect to assumptions about mechanistic details and aerosol concentration.

The PRE-INDOEX measurements showed large ozone diurnal variations both north and south of the ITCZ, even though the sulfate concentration were much higher in the NH than the SH [*Rhoads et al.*, 1997]. In addition, no rain was observed for the 6 days in the NHmE regime, but several rain events occurred during the 7 days in the SHmE regime. These results contrast somewhat with the model predictions and suggest that sulfate aerosols and dry weather are not necessary conditions for the generation of reactive bromine.

In the model with aerosol chemistry we assumed a constant O_3 flux of 2.2 x 10^{11} cm^{-2} s^{-1}, sufficient to maintain ozone levels near those observed. A variable rate of entrainment of ozone-rich air from the free troposphere can also contribute to diurnal variations, as suggested by *Bremaud et al.* [1998]. In their observations at Reunion, ozone concentrations began recovery around 2000 local time, but over the Indian Ocean we saw ozone concentrations begin to rise before nightfall, indicating that entrainment was active during the day. In the absence of measurements of ozone flux or profiles at night, we can only speculate on the impact of boundary layer dynamics. For an upper limit we assume no aerosol chemistry, with all the ozone flux at night. The difference between maximum and minimum is twice that shown on Figure 6 for no aerosols (base) or 24%. This is enough to contribute significantly to the diurnal variation but not sufficient to explain the 32% observed; both the meteorological and photochemical mechanisms are probably involved.

The natural rate of removal of ozone in the remote marine atmosphere may be faster than previously assumed. For the conditions observed over the Indian Ocean, the destruction rate was more than double that due to ozone photolysis and HO_x chemistry, but to understand the role of halogens in the global ozone budget, we must determine how frequently these condition occur. Further investigation of the role of halogens in tropospheric photochemistry should include measured bromide deficits on sea-salt aerosol; profiles of O_3 and H_2O (both day and night); and simultaneous observations of actinic UV flux, RO_2, and reactive halogens.

Acknowledgments. This work was supported by the NSF-funded Center for Clouds Chemistry and Climate as part of the INDOEX program and by NSF grants ATM9414846 and ATM9612893. The cruise was also supported by NOAA/AOML. The highly professional performance of the captain and crew of NOAA's Malcolm Baldrige are gratefully acknowledged. The authors wish to thank M. Farmer, W. Keene, R. Sander, and R. Vogt for useful advice and

P. Kelly, who helped collect the data. R. R. D. wishes to thank the MPI for support during his sabbatical leave and P. Ariya, C. Bruehl, and M. Lawrence for amiable guidance provided there.

References

Ariya, P. A., B. T. Jobson, R. Sander, H. Niki, G.W. Harris, and J. F. Hopper, Measurements of C_2 - C_7 hydrocarbons during the polar sunrise experiment 1994: Further evidence for halogen chemistry in the troposphere, *J. Geophys. Res., 103*, 13,169-13,180, 1998.

Bahe, F. C., W. N. Marx, U. Schurath, and E. P. Roth, Determination of the absolute photolysis rate of ozone by sunlight, $O_3 + h\nu \rightarrow O(^1D) + O_2(^1\Delta_g)$ at ground level, *Atmos. Environ., 13*, 1515-1522, 1979.

Bairai, S. T., and D. H. Stedman, Actinometric measurement of $j(O_3\text{-}O(^1D))$ using a Luminol detector, *Geophys. Res. Lett., 19*, 20047-2050, 1992.

Barrie, L. A., J. W. Bottenheim, P. J. Crutzen, and R. A. Rasmussen, Ozone destruction at polar sunrise in the lower Arctic atmosphere, *Nature, 334*, 138-141, 1988.

Blackburn, T. E., S. T. Bairai, and D. H. Stedman, Solar photolysis of ozone to singlet D oxygen atoms. *J. Geophys. Res., 97*, 10,109-10, 117, 1992.

Bremaud, P. J., F. Taupin, A. M. Thompson, and N. Chaumerliac, Ozone nighttime recovery in the marine boundary layer: Measurement and simulation of the ozone diurnal cycle at Reunion Island, *J. Geophys. Res., 103*, 3463-3473, 1998.

Chin, M., D. J. Jacob, G. M. Gardner, M. S. Foreman-Fowler, P. A. Spiro, and D. L. Savoie, A global three-dimensional model of tropospheric sulfate, *J. Geophys. Res., 101*, 18,667-18, 690, 1996.

Crutzen, P. J., A discussion of the chemistry of some minor constituents in the stratosphere and troposphere, *Pure Appl. Geophys., 106*, 1385-1399, 1973.

de Laat, A. T. J., M. Zachariasse, G. J. Roelofs, P. van Velthoven, R. R. Dickerson, K. P. Rhoads, S. J. Oltmans, and J. Lelieveld, Tropospheric O_3 distribution over the Indian Ocean during spring 1995, and evaluation of a chemistry-climate model, *J. Geophys. Res., 104*, 13,881-13,910, 1999.

Dickerson, R. R., D. H. Stedman, and A. C. Delany, Direct measurements of ozone and nitrogen dioxide photolysis rates in the troposphere, *J. Geophys. Res., 87*, 4933-4946, 1982.

Emmons, L. K., et al., Climatologies of NO_X and NO_Y: A comparison of data and models, *Atmos. Environ., 31*, 1837-1850, 1997.

Erickson, D. J., C. Seuzaret, W. C. Keene, and S. -L. Gong, A GCM-based model of HCl and $ClNO_2$ production from sea-salt dechlorination: The reactive chlorine emissions inventory, *J. Geophys. Res.*, in press, 1999.

Fan, S.-M. and D. J. Jacob, Surface ozone depletion in Arctic spring sustained by aerosol bromine reactions, *Nature*, 522-524, 1992.

Finlayson-Pitts, B. J., Comment on "Indications of photochemical histories of Pacific air masses from measurements of atmospheric trace species at Point Arena, California," *J. Geophys. Res., 98*, 14,991-14,993, 1993.

Graedel, T. E., and W. C. Keene, Tropospheric budget of reactive chlorine, *Global Biogeochem. Cycles, 9*, 47-77, 1995.

Hirokawa J. K. Onaka, Y. Kajii, and A. Akimoto, Heterogeneous processes involving sodium halide particles and ozone: Molecular bromine release in the marine boundary layer in the absence of nitrogen oxides, *Geophys. Res. Lett., 25*, 2449-2452, 1998.

Hofzumahaus, A., T. Brauers, U. Platt, and J. Callies, Latitudinal variation of measured photolysis frequencies $j(O^1D)$ and primary OH production rates over the Atlantic Ocean between 50°N and 30°S, *J. Atmos. Chem., 15*, 283-298, 1992.

Intergovernmental Panel on Climate Change (IPCC), Radiative Forcing of Climate Change. The 1994 report on the Scientific Assessment Working Group of IPCC, World Meteorol. Office, United Nations Environ. Programme, World Meteorol. Org., Geneva, 1994.

Jobson, B. T., H. Niki, Y. Yokouchi, J. Bottenheim, F. Hopper, and R. Leaitch, Measurements of C_2-C_6 hydrocarbons during the polar sunrise experiment: Evidence for Cl and Br atom chemistry, *J. Geophys. Res., 99, 25*,355-25,368, 1994.

Jobson, B. T., D. D. Parrish, P. Doldan, W. Kuster, F. C. Fehsenfeld, D. R. Blake, N. J. Blake, and H. Niki, Spatial and temporal variability of nonmethane hydrocarbons and their relation to photochemical lifetimes, *J. Geophys. Res., 103*, 13,557-13,567, 1998.

Johnson, J. E., R. H. Gammon, J. Larsen, T. S. Bates, S. J. Oltmans, and J. C. Farmer, Ozone in the marine boundary layer over the Pacific and Indian Oceans: Latitudinal gradients and diurnal cycles, *J. Geophys. Res., 95*, 11,847-11,856, 1990.

Keene, W. C., A. A. P. Pszenny, D. J. Jacob, R. A. Duce, J. N. Galloway, J. J. Schultz-Tokos, H. Sievering, and J. F. Boatman, The geochemical cycling of reactive chlorine through the marine troposphere, *Global Biogeochem. Cycles, 4*, 407-430, 1990.

Keene, W. C., D. J. Jacob, and S. M. Fan, Reactive chlorine: A potential sink for dimethylsulfide and hydrocarbons in the marine boundary layer, *Atmos. Environ., 30*, 1-3, 1996.

Keene, W. C., R. Sander, A. A. P. Pszenny, R. Vogt, P. J. Crutzen, and J. N. Galloway, Aerosol pH in the marine boundary layer: A review and model evaluation, *J. Aerosol Sci., 29*, 339-356, 1998.

Kim, J. H., R. D. Hudson, and A. M. Thompson, A new method of deriving time-averaged tropospheric column ozone over the tropics using total ozone mapping spectrometer (TOMS) radiances: Intercomparison and analysis using TRACE-A data, *J. Geophys. Res., 101*, 24,317-24,330, 1996.

Kley, D., P. J. Crutzen, H. G. J. Smit, H. Voemel, S. J. Oltmans, H. Grassl, and V. Ramanathan, Observations of near-zero ozone concentration over the convective Pacific: Effects on air chemistry, *Science, 274*, 230-233, 1996.

Lal, S., M. Naja, and A. Jayaraman, Ozone in the boundary layer over the tropical Indian Ocean, *J. Geophys. Res., 103*, 18,907-18,917, 1998.

Liu, S. C., D. Kley, M. McFarland, J. D. Mahlman, and H. Levy II, On the origin of tropospheric ozone, *J. Geophys. Res., 85*, 7546-7552, 1980.

McFarland, M., D. Kley, J. W. Drummond, A. L. Schmeltekopf, and R. H. Winkler, Nitric oxide measurements in the equatorial Pacific region, *Geophys. Res. Lett., 6*, 605-608, 1979.

McKeen, S. A. and S. C. Liu, Hydrocarbon ratios and the photochemical history of air masses, *Geophys. Res. Lett., 20*, 2363-2366, 1993.

McPeters, R. D., G. J. Labow, and B. J. Johnson, An SBUV ozone climatology for balloonsonde estimation of total column ozone, *J. Geophys. Res., 102*, 8875-8885, 1997.

Oltmans, S. J., Surface ozone measurements in clean air, *J. Geophys. Res., 86*, 1174-1180, 1981.

Oltmans, S. J., and H. Levy II, Surface ozone measurements from a global network, *Atmos. Environ. 28*, 9-24, 1994.

Oltmans, S. J., et al., Summer and spring profiles over the North Atlantic from ozonesonde measurements, *J. Geophys. Res., 101*. 29,179-29,200, 1996.

NASA/Jet Propulsion Laboratory (JPL), Chemical kinetics and photochemical data for use in stratospheric modeling *Eval., 12*, Pasadena, Calif., 1997.

Paluch, I. R., S. McKeen, D. H. Lenschow, R. D. Schillawski, and G. L. Kok, Evolution of the subtropical marine boundary layer: Photochemical ozone loss, *J. Atmos. Sci., 52*, 2967-2976, 1995.

Parrish, D. D., C. J. Hahn, E. J. Williams, R. B. Norton, F. C. Fehsenfeld, H. B. Singh, J. D. Shetter, B. W. Gandrud, and B. A. Ridley, Reply, *J. Geophys. Res., 98*, 14,995-14,997, 1993.

Piotrowicz, S. R., R. A. Rasmussen, K. J. Hanson, and C. J. Fischer, Ozone in the boundary layer of the equatorial Atlantic Ocean, *Tellus, Ser. B, 41B*, 314-322, 1989.

Pszenny, A. A. P., W. C. Keene, D. J. Jacob, S. Fan, J. R. Maben, M. P. Zetwo, M. Springer-Young, and J. N. Galloway, Evidence of inorganic Cl gases other than hydrogen chloride in marine surface air, *Geophys. Res. Lett., 20*, 699-702, 1993.

Ramanathan, V., et al., Indian Ocean Experiment (INDOEX) A multi-agency proposal for a field experiment in the Indian Ocean, C4, 83 pp., Scripps Inst. of Oceanogr., Univ. of Calif., San Diego, La Jolla, 1996.

Rhoads, K. P., The influence of continental emissions of the composition of the remote marine boundary layer, Ph.D. dissertation, Dept. of Chem., Univ. of MD, College Park, 1998.

Rhoads, K. P., P. Kelley, R. R. Dickerson, T. Carsey, M. Farmer, S. J. Oltmans, D. Savoie, and J. M. Prospero, The composition of the troposphere over the Indian Ocean during the monsoonal transition, *J. Geophys. Res. 102*, 18,981-18,995, 1997.

Sander, R., and P. J. Crutzen, Modeling the chemistry of ozone, halogen compounds, and hydrocarbons in the arctic troposphere during spring, *Tellus, Ser. B, 49*, 522-532.

Sander, R., R. von Glasow, and P. J. Crutzen. Modeling the chemistry of ozone and halogen compounds, in the remote marine boundary layer, *Ann. Geophys*, suppl. II, *16*, C721, 1998.

Shetter, R. E., et al., Actinometric and radiometric measurement and modeling of the photolysis rate coefficient of ozone to $O(^1D)$ during Mauna Loa Observatory Photochemical Experiment 2, *J. Geophys. Res.*, *101*, 14,631-14,641, 1996.

Singh, H. B., et al., Low ozone in the marine boundary layer of the tropical Pacific Ocean: Photochemical loss, chlorine atoms and entrainment, *J. Geophys. Res.*, *101*, 1907-1917, 1996.

Spicer, C. W., E. G. Chapman, B. J. Finlayson-Pitts, R. A. Plastridge, J. M. Hubbe, J. D. Fast, and C. M. Berkowitz, First observations of Cl_2 and Br_2 in the marine troposphere, *Nature*, *394*, 353, 1998.

Suhre, K., M. O. Andreae, and R. Rosset, Biogenic sulfur emissions and aerosols over the tropical South Atlantic 2, One dimensional simulation of sulfur chemistry in the marine boundary layer, *J. Geophys. Res.*, *100*, 11,323-11,334, 1995.

Thompson, A. M., et al., SAGA-3 ozone observations and a photochemical model analysis of the marine boundary layer during SAGA-3, *J. Geophys. Res.*, *98*, 16,955-16,968, 1993.

Torres, A. L., and A. M. Thompson, Nitric oxide in the equatorial Pacific boundary layer: SAGA-3 measurements, *J. Geophys. Res.*, *98*, 16,949-16,953, 1993.

Vogt, R., P. J. Crutzen, and R. Sander, A mechanism for halogen release from sea salt aerosol in the remote marine boundary layer, *Nature*, *383*, 327-330, 1996.

Vogt, R., R. Sander, R. von Glasow, and P. J. Crutzen, Iodine chemistry and halogen activation in the marine boundary layer: A model study, *J. Atmos. Chem.*, *32*, 375-395, 1999.

Yvon, S. A., E. S. Saltzman, D. J. Cooper, T. S. Bates, and A. M. Thompson, Atmospheric sulfur cycling in the tropical Pacific marine boundary layer (12°S, 135°W): A comparison of field data and model results, 1, Dimethylsulfide, *J. Geophys. Res*, *101*, 6899-6901, 1996.

Wingenter, O. W., M. K. Kugo, N. J. Blake, T. W. Smith, D. R. Blake, and F. S. Rowland, Hydrocarbon and halocarbon measurements as photochemical and dynamical indicators of atmospheric hydroxyl, atomic chlorine, and vertical mixing obtained during Lagrangian flights, *J. Geophys. Res.*, *101*, 4331-4340, 1996.

J. P. Burrows, Institut für Umweltphysik (Fernerkundung, Universitäet Bremen, FBI, Postfach 330440, 28334 Bremen, Germany.

T. P. Carsey, Atlantic Oceanographic and Meteorological Laboratory, NOAA, Ocean Chemistry Division, 4301 Rickenbacker Causeway, Miami, FL 33149.

P.J. Crutzen, Abteilung Luftchemie, Max Planck Institut für Chemie 55020 Mainz, Germany.

R. R. Dickerson and K. P. Rhoads, Departments of Meteorology and Chemistry, University of Maryland, 3433 CSS Building, College Park, MD 20742. (russ@atmos.umd.edu).

S. J. Oltmans, Climate Monitoring and Diagnostics Laboratory, NOAA, 325 Broadway, Boulder, CO 80303.

(Received August 25, 1998; revised December 11, 1998, accepted January 13, 1999.)